Clinical and molecular characterization of a family with a dominant renin gene mutation and response to treatment with fludrocortisone

A.J. Bleyer[1,*], **M. Živná**[2,3,*], **H. Hulková**[3], **K. Hodanová**[2,3], **P. Vyletal**[2,3], **J. Sikora**[3], **J. Živný**[4], **J. Sovová**[3], **T.C. Hart**[5], **J.N. Adams**[6], **M. Elleder**[2,3], **K. Kapp**[7], **R. Haws**[8], **L.D. Cornell**[9], **S. Kmoch**[2,3], and **P.S. Hart**[6]

[1]Section on Nephrology, Wake Forest University School of Medicine, Winston-Salem, NC, USA

[2]Center for Applied Genomics, Charles University in Prague, First Faculty of Medicine, Prague, Czech Republic

[3]Institute for Inherited Metabolic Disorders, Charles University in Prague, First Faculty of Medicine, Prague, Czech Republic

[4]Institute of Pathophysiology, Charles University in Prague, First Faculty of Medicine, Prague, Czech Republic

[5]Human Craniofacial Genetics Section, NIDCR, NIH

[6]Office of the Clinical Director, National Human Genome Research Institute, National Institutes of Health, Bethesda, MD, USA

[7]ZMBH (Center for Molecular Biology Heidelberg), University of Heidelberg, Heidelberg, Germany

[8]Specialty Pediatrics, Marshfield, WI

[9]Division of Anatomic Pathology, Department of Laboratory Medicine and Pathology, Mayo Clinic, Rochester, MN, USA

Abstract

Background—A family was identified with autosomal dominant inheritance of anemia, polyuria, hyperuricemia, and chronic kidney disease. Mutational analysis revealed a novel heterozygous mutation c.58T > C resulting in the amino acid substitution of cysteine for arginine in the preprorenin signal sequence (p.cys20Arg) occurring in all affected members.

Methods—Effects of the identified mutation were characterized using in vitro and in vivo studies. Affected individuals were clinically characterized before and after administration of fludrocortisone.

Results—The mutation affects endoplasmic reticulum co-translational translocation and posttranslational processing, resulting in massive accumulation of non-glycosylated preprorenin in

Correspondence to A.J. Bleyer, MD, Section on Nephrology, Wake Forest University School of Medicine, Medical Center Blvd., Winston-Salem, NC 27157, USA, ableyer@wfubmc.edu.
*These authors contributed equally.

the cytoplasm. This affects expression of intra-renal RAS components and leads to ultrastructural damage of the kidney. Affected individuals suffered from anemia, hyperuricemia, decreased urinary concentrating ability, and progressive chronic kidney disease. Treatment with fludrocortisone in an affected 10-year-old child resulted in an increase in blood pressure and estimated glomerular filtration rate.

Conclusions—A novel *REN* gene mutation resulted in an alteration in the amino acid sequence of the renin signal sequence and caused childhood anemia, polyuria, and kidney disease. Treatment with fludrocortisone improved renal function in an affected child. Nephrologists should consider *REN* mutational analysis in families with autosomal dominant inheritance of chronic kidney disease, especially if they suffer from anemia, hyperuricemia, and polyuria in childhood.

Keywords

Introduction

Autosomal dominant interstitial kidney disease associated with hyperuricemia has previously been attributed to mutations in the *UMOD* gene [1], which produces uromodulin. Recently, mutations in the gene encoding renin were identified as a cause of hereditary interstitial kidney disease associated with hyperuricemia [2]. These mutations resulted either in the deletion (p.Leu16del) or the amino acid exchange (p.Leu16Arg) of a single leucine residue located in the hydrophobic portion (h-region) of the renin signal sequence. This region of the protein is essential for efficient co-translational translocation of the synthesized preprorenin into the endoplasmic reticulum (ER), where glycosylation and proteolytic processing of the nascent preprorenin occur and condition further transit of prorenin and renin through the secretory pathway [3].

In this investigation, we describe a family with a novel *REN* mutation affecting the polar C-terminal portion (c-region) of the preprorenin signal sequence and resulting in an autosomal dominant clinical syndrome characterized by decreased plasma renin levels, polyuria, anemia, hyperuricemia, and progressive kidney failure. We describe how the mutation modifies the biosynthesis of prorenin and renin, the effects of the mutation at the cellular level, and the pathophysiologic changes that result from the mutation. For the first time we describe treatment of this condition with fludrocortisone.

Methods

The procedures were approved by the Wake Forest University School of Medicine Institutional Review Board.

Patient ascertainment

The family was referred by RH for evaluation of anemia, polyuria, and chronic kidney disease. Blood and urine samples were obtained for chemical and genetic analysis, and a retrospective review of medical records was performed. DNA samples were collected on family members, and mutational analysis of the *REN* gene was performed.

In affected individuals, 24 h urine collections were performed on an ad libitum diet for urinary electrolytes and aldosterone. Random plasma renin and aldosterone levels were determined. When one of the patients (AIII2) (Figure 1A) was identified as having hypoaldosteronism, the patient's nephrologist started her on fludrocortisone acetate, 0.1 mg orally each day. Two other affected individuals (AII6 and an unrelated individual with a heterozygous deletion p.Leu16del in the *REN* gene characterized in our previous study (BII4 [2])) were enrolled in a protocol in which baseline blood and urine samples were obtained, and participants were then placed on 3 days of fludrocortisone at a dosage of 0.1 mg orally each day, followed by fludrocortisone at a dosage of 0.2 mg orally for 4 days.

Sequence analysis and genotyping

The *REN* gene was PCR amplified from genomic DNA and sequenced in AII6, AIII2, and clinically unaffected family members using methods previously described [2]. The presence of a novel *REN* mutation was evaluated in the complete family and in a control European American population (n = 385) by direct sequencing. A set of microsatellite markers flanking the *REN* locus were genotyped to identify the disease associated haplotype segregating with the novel *REN* mutation.

Laboratory investigation

In silico analysis—Preprorenin signal sequences from the presented species were obtained from the UniProtKB/Swiss-Prot database. Multiple alignment and evaluation for amino acid conservation were performed by ClustalW2 software (http://www.ebi.ac.uk/Tools/clustalw2/). Properties of the signal sequences were assessed using the SignalP 3.0 server [4] and the Kyte and Doolittle method [5].

In vitro translation/translocation and transient expression of the p.Cys20Arg preprorenin—Construction of the wild-type preprorenin (WT^{REN}) eukaryotic expression vector was performed as previously described [2]. The mutant construct c.58T > C, encoding the p.Cys20Arg preprorenin (C20R^{REN}), was prepared by site directed mutagenesis of the WT^{REN} vector using a mutation specific oligonucleotide primer and the GeneTailor™ Site – Directed Mutagenesis System Kit (Invitrogen, Paisley, UK).

In vitro translation/ translocation assays, transient transfection of human embryonic kidney (HEK293) cells, culturing conditions, cell lysate preparation, media collection, and Western blot and immunofluorescence analyses of prorenin and renin were carried out as previously described [2].

Renin granulosity was assessed by the fluorescence-activated cell sorter (FACS) assay, measuring the differences in the fluorescence intensity and the number of granular cells after the transient transfection of HEK293 cells with WT^{REN}, C20R^{REN} and empty pCR3.1 expression vectors and labeling of low pH secretory granules with fluorescent amino-acridine dye quinacrine. For this assay, 8×10^5 HEK293 cells were transfected with 4 µg of the corresponding vectors. Cells were mechanically harvested 24 h post-transfection using 1.2 ml of supplemented Dulbecco's Modified Eagle's Medium (DMEM) without phenol red. Five minutes before the analysis, 400 µl of 8 µM quinacrine dihydrochloride (Sigma,

Prague, Czech Republic) in DMEM without phenol red was added to 400 μl of the cell suspension containing approximately 500,000 cells. Fluorescence was measured using FACS Calibur flow cytometer, and data were analyzed using Cell Quest software version 3.3. (Becton Dickinson, San Jose, Ca, USA). The quinacrine positive cells, i.e. cells containing acidic granules, were gated and analyzed for their granularity by measurement of side scatter intensity. The cells with high side scatter intensity, i.e. more granular cells, were counted. The number of low-pH granules was quantified as the mean fluorescence intensity (MFI) of gated quinacrine positive population of 100,000 cells.

Light microscopy, immunohistochemistry and electron microscopy studies—
A kidney biopsy of patient AII6 was performed; the tissue sample was processed as previously described [6]. Selected antigens were investigated using the following primary antibodies: protenin + renin – rabbit anti-preprorenin (amino acid residues 288 – 317), (Yanaihara, Shizuoka, Japan); angiotensin converting enzyme 1, mouse anti-angiotensin converting enzyme 1 antibody (Abcam, Cambridge, UK); angiotensin II, mouse anti-angiotensin II antibody (Acris, Herford, Germany); uromodulin, rabbit anti-Tamm-Horsfall protein antibody (Biogenesis, Poole, UK).

Ultrastructural studies were performed on deparaffinized tissue from the material originally submitted for light microscopy. Thin sections were double contrasted with uranyl acetate and lead nitrate and examined using Jeol 1200 EX electron microscope.

Results

Clinical findings

Patient AIII2—The proband was the product of a 38 week gestation and weighed 3.19 kg at birth. She presented with acute kidney failure at 3 years. The patient had suffered from a viral syndrome with fevers up to 38.9 °C and was placed on non-steroidal anti-inflammatory agents (NSAIDs). Laboratory studies revealed a blood urea nitrogen (BUN) of 25.3 mmol/l (71 mg/dl) (normal range 1.8 – 6.4 mmol/l), serum creatinine 124 umol/l (1.4 mg/dl) (normal 37.2 – 50.4 umol/l), and hemoglobin 76 g/l (normal 115 – 135 g/l). Acute kidney failure was attributed to NSAIDs, which were stopped with a decline in the serum creatinine to 71 umol/l (0.8 mg/dl). The patient was evaluated at age 6 years for a persistently elevated serum creatinine level of 106 umol/l (1.2 mg/dl). The patient was asymptomatic except for nocturia.

On physical examination the patient appeared her stated age, with height 118.5 cm and weight 22.7 kg. The blood pressure was 82/52 mmHg with pulse 86 beats per minute. The rest of the physical examination was unremarkable. With renal ultrasound, the right kidney was 7 cm and the left kidney 8.5 cm (normal for age 8.5 – 11.5 cm) without any cysts. A computerized axial tomographic scan revealed no cysts. The serum sodium was 141 mmol/l, potassium 5.5 mmol/l, chloride 106 mmol/l, bicarbonate 23 mmol/l, BUN 19.6 mmol/l, and serum creatinine 106.1 umol/l. The serum uric acid was elevated at 375 umol/l (6.3 mg/dl) (normal range 107 – 315 umol/l), with a fractional excretion of uric acid (FE_{urate}) 5.2% (normal 6 – 20%). A 24 h urine collection revealed 6.3 mg/m^2/h protein (normal < 4 mg/m^2/h), urine sodium 5.2 mEq/kg/day, and volume 57 ml/kg. The creatinine clearance

was 58 ml/min/1.73 m^2. The hemoglobin level was low at 105 g/l, with a mean corpuscular volume of 76 fl (normal 82 – 98 fl) and a mean cell hemoglobin of 25.5 pg (normal 25.5 – 34.5 pg), with an iron saturation of 5%, ferritin 135 ng/ml, and erythropoietin level 3.2 mIU/ml (normal 4 – 21 mIU/ml).

Anemia: The patient was started on iron replacement and darbepoeitin α at age 7. With intravenous iron administration, the patient achieved full repletion of her iron stores (iron saturation 33% and ferritin 541 ng/ml), but she has subsequently remained dependent on darbepoeitin α therapy to maintain hemoglobin levels above 110 g/l to the present age of 11 years.

Hyperuricemia: The patient's serum uric acid remained elevated, rising to 458 umol/l (7.7 mg/dl) at age 7. The FEurate remained low with readings less than 5.2%, and the lowest reading of 3.2%.

Renin/aldosterone: A random plasma renin activity was < 0.5 ng/ml/h (normal 0.5 – 5.9 ng/ml/h) with a random serum aldosterone measurement < 4.0 ng/dl at age 10 years (normal 4 – 31 ng/dl). A 24 h urine aldosterone was 2 μg/24 h (normal 2 – 16 μg/24 h).

Treatment with fludrocortisone: Based on the findings of hyporeninemic hypoaldosteronism, the patient was started on treatment with fludrocortisone, 0.1 mg orally each day at age 10 years. The eGFR showed a significant increase with administration of fludrocortisone (Figure 2), which was sustained (Table 1).

Urinary concentration: Overnight urinary osmolality (with fasting from 10 pm to 8 am), was 386 mOsm/kg while receiving fludrocortisone. Two hours later, with continued fasting, the urine osmolality was 377 mOsm/kg. A repeat measurement was performed 4 months after fludrocortisone therapy. At that time the overnight urine osmolality remained at 386 mOsm/kg.

Patient AII6—The proband's father presented at age 14 years for unexplained anemia with a hemoglobin 93 g/l, white blood count 5,000/ml, and platelet count 101,000/ml. Bone marrow aspirate revealed normoblastic hypoplasia. The patient was diagnosed with hypoplasia of the bone marrow, cause unknown. As part of the evaluation, an intravenous urogram revealed the left kidney to be 12.8 cm and the right kidney 11.3 cm. The serum creatinine was elevated at 115 umol/l (1.3 mg/dl). The hemoglobin increased to 114 g/l 3 months later without treatment. Follow-up for this problem was limited thereafter, without any hemoglobin values available until adulthood.

The patient was diagnosed with gout at age 29 years and placed on allopurinol. The patient was not overweight at the time and did not have excessive alcohol consumption or other risk factors.

At age 33 years the patient was referred to a nephrologist. On physical examination, the height was 185 cm, weight 85 kg, blood pressure 112/78 mmHg, and pulse 52 beats per minute. The urinalysis was bland. The serum sodium was 143 mmol/l, potassium 4.7

mmol/l, BUN 16.4 mg/dl, serum uric acid level (on allopurinol) 381 umol/l (6.4 mg/dl). The hemoglobin was 153 g/l, platelet count 108,000/ml. The 24 h creatinine clearance was 75 ml/min with 2.25 liters and 245 mg protein. A CT scan revealed no renal lesions, without comment on kidney size.

A kidney biopsy (Figure 3) revealed periglomerular fibrosis without other glomerular abnormalities. There was tubular atrophy with marked thickening of tubular basement membranes in the cortex, and interstitial fibrosis accompanied by a focal mild interstitial inflammatory infiltrate composed of mononuclear cells. No tubulitis was identified. Tubular atrophy was present in the medulla, which contained focally dilated and atrophic tubules with flattened epithelium and atypical proteinaceous casts. The juxtaglomerular apparatus was not prominent.

Electron microscopy (Figure 4) revealed one complete glomerulus and one partial glomerulus that showed a thickened Bowman's capsule. Glomerular basement membranes were thickened; no basement membrane duplication, lamellations, or microparticles were identified. Podocytes showed mild segmental foot process effacement; otherwise, podocytes did not display any significant alterations (Figure 4A). The mesangium was unremarkable. No electron dense deposits were identified. The most prominent ultrastructural changes in the nephron were marked distention of basal membrane invaginations in both proximal tubules (PT) (Figure 4B,D) and distal tubules (DT), with marked distension of the intercellular space in the latter (Figure 4C). The tubular basement membranes were thickened (Figure 4B,C,D). Generally there was a marked tendency of PT epithelium to atrophy, without any significant reduction of the brush border, however (Figure 4D). Tubules were lined by atrophic epithelium with luminal distension by cell debris. Peritubular capillaries did not reveal any ultrastructural abnormalities. There was no sign of distension of the endoplasmic reticulum. There were no noted structural abnormalities of mitochondria, which were frequently packed. The lysosomes in PT were distended with various amounts of protein. The population of peroxisomes was not well discernible.

Further testing was performed at age 42 years. The erythropoietin level was 18.5 mIu/ml (normal 4.1 – 19.5 mIu/ml). A 24 h urine collection was 3,450 ml, with 283 mEq sodium, and 111 mEq potassium. The FE_{urate} was 3.6% (normal 5 – 20%). The 24 h urinary aldosterone excretion was 9 ug/24 h (normal 2 – 21 ug/24 h on a regular salt diet and 17 – 44 ug/24 h on a low sodium diet).

Urinary concentration: Urinary osmolality was 426 mOsm/kg after an overnight fast, and 2 h later was 427 mOsm/kg with continued fasting (Table 2).

Chronic kidney failure: eGFR has remained stable over time (Figure 2).

Mutational analysis: Sequencing of the *REN* gene revealed a novel heterozygous mutation c.58T > C, resulting in the amino acid substitution p.Cys20Arg, (C20R[REN]) in the proband (AIII2) and her affected father (AII6) (Figure 1B). The mutation arose de novo in AII6 on the maternal haplotype and was not present in any unaffected family members, even AII3

and AII5 who inherited the same maternal haplotype. The mutation was not present in 385 unrelated Caucasian controls (770 alleles).

Fludrocortisone administration: Patients AII6 and patient BII4 from a family with the mutation p.Leu16del [2] received fludrocortisone as part of the protocol described in the Methods. There was no effect on hemodynamics or eGFR in these patients. The FE_{urate} did not change in any participants. Urine volume did not decrease with fludrocortisone administration.

Laboratory investigations

In silico analysis: Human prorenin and renin are synthesized in juxtaglomerular cells from a preproprotein composed of a 23 residue N-terminal signal sequence, which mediates insertion of the nascent preproprotein into the translocation channel within the ER membrane, a 43 residue "pro" domain, and the mature enzymatically active renin comprising 340 residues [7]. In contrast to the previously reported p.Leu16del and p.Leu16Arg mutations, which are located within the hydrophobic part of the signal sequence (h-region) and affect protein insertion in the ER membrane, the p.Cys20Arg mutation occurs in the polar C-terminal part (c-region) of the preprorenin signal sequence. This cysteine residue is conserved among mammals except for sheep (Figure 5A). Using the SignalP3.0 server [4], the p.Cys20Arg mutation decreases the overall hydrophobicity profile of the c-region of the signal sequence (Figure 5B) and alters its cleavage site score profile and cleavage site probability.

Characterization of the p.Cys20Arg preprorenin: WT^{REN} and $C20R^{REN}$ proteins were transfected and ER-translocated in vitro (Figure 5C) and transiently expressed in HEK 293 cells (Figure 6). Densitometry analysis of 5 replicate experiments (Figure 5C) revealed that on average $56 \pm 6\%$ of WT^{REN} protein is converted to glycosylated prorenin (ProREN) in the presence of rough ER microsomes, whereas conversion of $C20R^{REN}$ to ProREN is reduced to $23 \pm 5\% (p < 0.01)$. WT^{REN} and $C20R^{REN}$ proteins were repeatedly (n = 3) transiently expressed in HEK 293 cells, and expressed proteins were detected in cell lysates and medium by Western blot analysis (Figure 6A). In lysates, the WT^{REN} was expressed as a 47 kDa protein whereas the $C20R^{REN}$ was expressed as a 45 kDa protein. Deglycosylation with PNGase reduced the molecular weight of the WT^{REN} to 43 kDa, corresponding to complete loss of N-glycosylation on both of the predicted N-glycosylation sites in the preprorenin sequence (N71 and N141). The molecular weight of $C20R^{REN}$ remained unchanged. Analysis of molecular weights suggests that WT^{REN} produces the fully glycosylated prorenin (ProREN), and that this protein has successfully completed ER translocation and undergone cleavage of its signal sequence, whereas $C20R^{REN}$ produces only non-glycosylated preprorenin (PreProREN). Analysis of the medium showed, however, that the $C20R^{REN}$ protein produces also minute amounts of glycosylated, proteolytically processed and therefore secretory competent prorenin. Immunofluorescence analysis (Figure 6C,D) demonstrated that compared to the WT^{REN}, the $C20R^{REN}$ protein does not form cytoplasmic granules and instead has intense diffuse cytoplasmic staining.

Inability of C20R^{REN} to form cytoplasmic granules was confirmed by the FACS based assay. This assay showed that, similar to mock transfection, the expression of C20R^{REN} does not increase either the number of granular cells (Figure 6B), or the quinacrine fluorescence (data not shown) as is the case in cells expressing the WT^{REN} protein.

Expression of uromodulin and intrarenal RAS components in kidney:

Immunohistochemistry analysis (Figure 7) revealed no renin positive cells (unfortunately, only one glomerulus was present in the tissue section). As for the other local kidney RAS components, angiotensin converting enzyme 1 (ACE 1) (Figure 7A,B) and angiotensin II (ANG II) (Figure 7C,D) revealed irregular staining which was in relatively preserved tubules comparable with age matched controls. Uromodulin (UMOD) staining (Figure 7E,F) was decreased but present on the apical membrane of TALH cells as in controls.

Discussion

In this study we identified a family with a novel mutation in the REN gene resulting in the autosomal dominant inheritance of early onset anemia, polyuria, hyperuricemia, and slowly progressive chronic kidney disease. In this family the mutation arose de novo in the proband's father. The identified mutation affects the signal sequence properties and function as shown by bioinformatic analysis, in vitro translation/translocation studies and transient expression and characterization of the mutant protein. These studies demonstrated that the mutation significantly decreased ER cotranslational translocation and post-translational processing of the mutant nascent protein, leading to massive accumulation of non-glycosylated preprorenin in cytoplasm. In contrast to the previously identified p.Leu16del and p.Leu16Arg mutations [2] which affected the h-region of the signal sequence, the novel mutation affects the c-region of the signal sequence and alters its cleavage site score profile and cleavage site probability. The insertion of a positively charged amino acid likely leads to the decreased translocation. This substitution also prevents renin granule formation (which occurred with the other mutations), a difference which may be responsible for the phenotypic differences seen in the affected families. Interestingly, affected members of all four families that have been described with this condition have had a mutation in the signal sequence of renin [2].

Mutations in the *REN* gene altering the renin signal peptide have three major effects: First, production of normal renin is markedly reduced in juxtaglomerular cells. Individuals with this disorder have low renin levels, low aldosterone levels, and frequently suffer from mild hyperkalemia. Second, the renin signal sequence-derived peptide is not present in the mutated cells due to aberrant preprotein processing. This may be important because the wild-type renin signal peptide exhibits uncommon stability and resistance to signal peptide peptidase processing, suggesting that it may have a post-targeting function [2]. Third, non-processed preprorenin is produced and accumulates intracellularly, presumably leading to the unfolded protein response, accelerated apoptosis, subsequent nephron loss, and progressive chronic kidney disease. It is clear that the patients are able to produce some renin, encoded and synthesized from the second unaffected allele. Individuals with genetic mutations resulting in total absence of renin production present with renal tubular dysgenesis and die either in utero or early in life [8].

The low renin production manifested itself early on in AIII2 when the patient developed acute kidney failure in the setting of a viral illness together with treatment with non-steroidal anti-inflammatory medications. The decreased renin production likely resulted in the inability to preserve intraglomerular pressure in the setting of volume depletion, and the non-steroidal medication aggravated this problem through inhibition of prostaglandin synthesis. Patients with this disorder should be advised to avoid non-steroidals and volume depletion, similar to individuals receiving angiotensin converting enzyme inhibitors.

Polyuria was a significant finding in the studied family and has not been seen in other families with this condition. Affected family members could not concentrate their urine after an overnight fast. These findings were very similar to the characteristics of mice that undergo Ren1c disruption [9], resulting in the inability to produce renin in the homozygous state. These mice suffer from polyuria and hypotension, with 80% of mice not surviving the first few days of life without salt repletion. These mice also manifest decreased weight, hypotension, and renal failure. Polyuria in these mice is resistant to desmopressin acetate (DDAVP) and unresponsive to angiotensin infusion. In our patients, fludrocortisone administration did not decrease urinary volume. The link between the renin angiotensin system and urinary concentration requires further investigation and has not been fully appreciated in the past.

Anemia has been observed in all children identified with *REN* mutations [2]. The anemia begins early in life, and hemoglobin values are characteristically between 100 and 120 g/l. The renin angiotensin system is known to affect erythropoiesis. Angiotensin II receptors have been identified on erythroid progenitors [10], and angiotensin II stimulates proliferation of normal early erythroid progenitors [11]. The anemia resolves once children enter the teenage years, but then recurs with advancing kidney failure. Production of androgens with puberty is well known to affect hematopoiesis [12] and may compensate for the decreased effect of the renin angiotensin system on hematopoiesis early in life.

Hyperuricemia is likely the result of increased proximal tubular reabsorption of urate. The relative hypotension associated with the low renin state likely stimulates proximal tubular sodium reabsorption, which secondarily results in increased proximal tubular urate reabsorption [13]. This mechanism would be analogous to that of patients with mutations in the gene encoding uromodulin [14] or in individuals with volume depletion [13].

Decreased uromodulin production potentially results directly from pathophysiologic changes occurring in the kidney as a result of the *REN* mutation. Based on our observations, we hypothesize that the renin signal sequence mutations expose juxtaglomerular cells, sustaining the highest expression of the mutant protein, to chronic ER stress and lead to site-specific attenuation of renin biosynthesis and renin angiotensin system (RAS) dysregulation. Reduced viability of juxtaglomerular cells and limited renin availability then affect renal development, intra-renal RAS homeostasis and kidney autoregulation. Over time, accelerated apoptosis occurs in juxtaglomerular cells in a similar manner to mice with ablated juxtaglomerular cells [15], leading to nephron loss and progressive kidney failure. Accelerated stress or even damage of tubular cells – exclusive producers of UMOD-leads (as in other tubulointerstitial kidney diseases) to reduced synthesis of major secretory

proteins which manifests with the reduced kidney expression and urinary excretion of UMOD as well as altered expression of mucin-1 protein (MUC1) [16] and other proteins. Reduced uromodulin in the mutant kidney could also be related to decreased intra-renal angiotensin expression. Lower angiotensin levels likely decrease uromodulin expression, as angiotensin converting enzyme inhibitors have been found to decrease urinary uromodulin excretion[17]. The low renin state results in relative hypotension simulating a low extracellular volume clinical state, which correlates with decreased uromodulin production in rats [18].

Chronic kidney failure appears to be very slow in progression, and is likely due to cell death in the setting of progressive intracellular accumulation of abnormal renin. However, the low renin levels likely provide continuous inhibition of aldosterone production and may paradoxically prevent renal failure from worsening.

If the production of abnormal renin leads to cell injury, decreasing production of renin (and hence abnormal renin) might be beneficial in preserving renal function in the long term. Since aldosterone has feedback inhibition on renin secretion, administration of aldosterone should decrease renin production and hence production of abnormal renin. In addition, patients suffer from polyuria, mild hypotension, and hyperkalemia, and fludrocortisone administration might reverse these conditions. Therefore, a trial of fludrocortisone was initiated in 3 patients. In the 10-year-old patient AIII2, fludrocortisone resulted in a decrease in serum potassium, a rise in blood pressure, and a significant improvement in estimated GFR that persisted over 6 weeks of administration. However, its administration had little effect on FE_{urate} or on the polyuria present in this patient. In the 2 adult patients, a one week trial of fludrocortisone had little effect. This may be due to the short duration of the study or the presence of irreversible changes in the kidney at this later stage of disease. The potential benefit of fludrocortisone to decrease production of abnormal renin in these patients must be weighed against potential harmful effects of aldosterone in chronic kidney disease.

This family has a number of clinical similarities and differences compared with the other families described with this disorder. All families described to date have suffered from chronic kidney disease, childhood anemia, and hypouricosuric hyperuricemia. In addition, this family suffered from polyuria and mild hypotension. Weaknesses of this study include the small number of patients in whom fludrocortisone was administered, making it very difficult to provide any firm conclusions. We were of course limited by the very small number of identified families. We plan to pursue investigations with fludrocortisone when more families are diagnosed with this disorder.

In summary, a novel dominant mutation in the *REN* gene is described that results in polyuria, anemia, hypouricosuric hyperuricemia, chronic kidney disease, and manifestations of hypoaldosteronism. Laboratory studies revealed that the mutation affected translocation of preprorenin into the ER with a marked decrease in synthesis of renin, and intracellular accumulation of abnormal renin. These findings are consistent with experimental findings for other *REN* mutations [2]. Treatment with fludrocortisone improved renal function and blood pressure in a child with this condition. Further research will concentrate on the effect

of prolonged fludrocortisone treatment in these patients. Patients with this condition should avoid non-steroidal anti-inflammatory agents and volume depletion.

The authors are very interested in performing mutational analysis in similar families and would be happy to receive communication by e-mail in this regard.
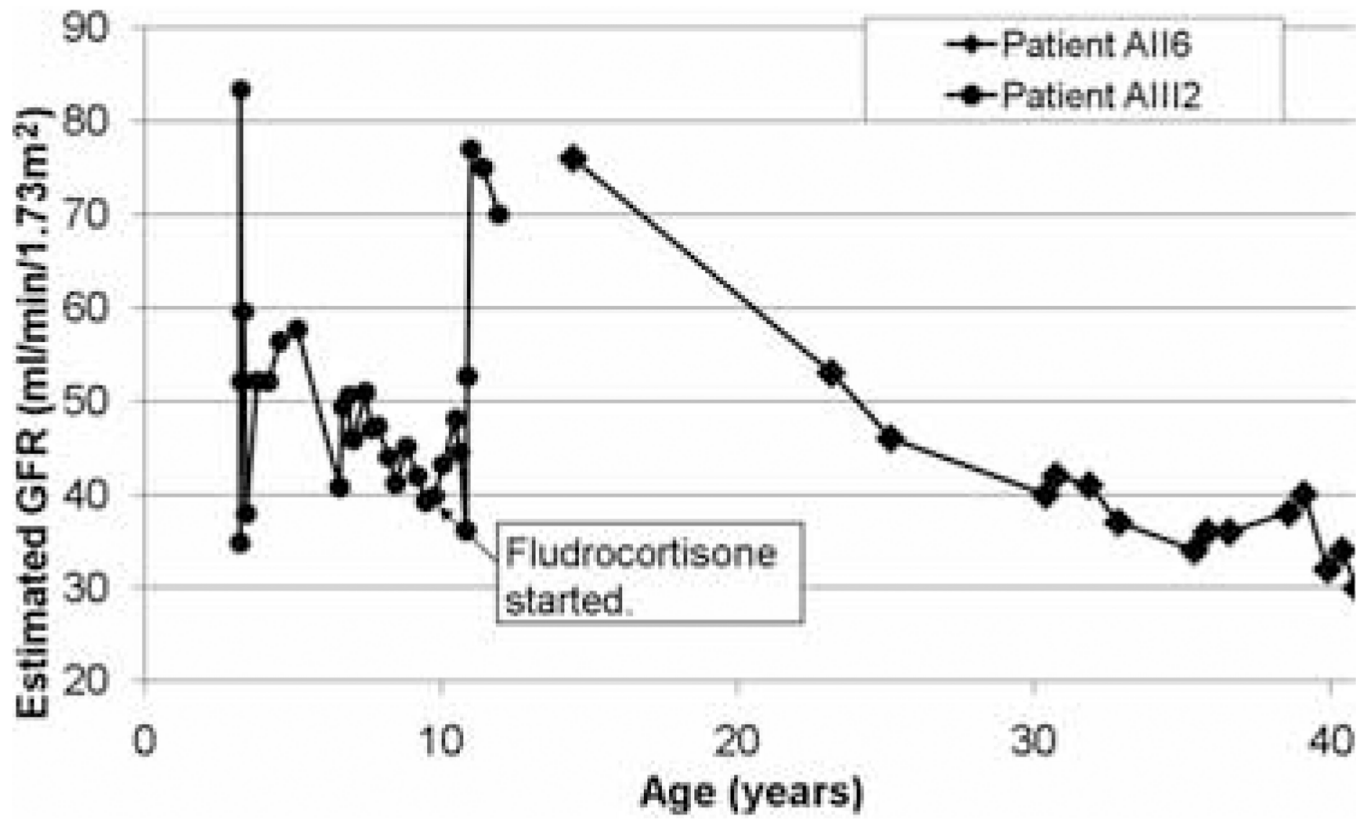
Acknowledgment

References

1. Hart TC, Gorry MC, Hart PS, et al. Mutations of the UMOD gene are responsible for medullary cystic kidney disease 2 and familial juvenile hyperuricaemic nephropathy. J Med Genet. 2002; 39:882–892. [PubMed: 12471200]

2. Zivna M, Hulkova H, Marignon M, et al. Dominant renin gene mutations associated with early-onset hyperuricemia, anemia, and chronic kidney failure. Am J Human Genet. 2009; 85:204–213. [PubMed: 19664745]

3. Imai T, Miyazaki H, Hirose S, et al. Cloning and sequence analysis of cDNA for human renin precursor. Proc Natl Acad Sci. 1983; 80:7405–7409. [PubMed: 6324167]

4. Bendtsen JD, Nielsen H, von Heijne G, Brunak S. Improved prediction of signal peptides: SignalP 3.0. J Mol Biol. 2004; 340:783–795. [PubMed: 15223320]

5. Kyte J, Doolittle RF. A simple method for displaying the hydropathic character of a protein. J Mol Biol. 1982; 157:105–132. [PubMed: 7108955]

6. Hodanova K, Majewski J, Kublova M, et al. Mapping of a new candidate locus for uromodulin associated kidney disease to chromosome 1q41. Kidney Int. 2005; 68:1472–1482. [PubMed: 16164624]

7. Hegde RS, Bernstein HD. The surprising complexity of signal sequences. Trends Biochem Sci. 2006; 31:563–571. [PubMed: 16919958]

8. Gribouval O, Gonzales M, Neuhaus T, et al. Mutations in genes in the renin-angiotensin system are associated with autosomal recessive renal tubular dysgenesis. Nat Genet. 2005; 37:964–968. [PubMed: 16116425]

9. Takahashi N, Sequeira Lopez ML, Cowhig JE, et al. Ren1c homozygous null mice are hypotensive and polyuric, but heterozygotes are indistinguishable from wild-type. J Am Soc Nephrol. 2004; 16:125–132. [PubMed: 15563565]

10. Mrug M, Julian BA, Prchal JT. Angiotensin II receptor type 1 expression in erythroid progenitors: Implications for the pathogenesis of postrenal transplant erythrocytosis. Semin Nephrol. 2004; 24:120–130. [PubMed: 15017524]

11. Mrug M, Stopka T, Julian BA, et al. Angiotensin II stimulates proliferation of normal early erythroid progenitors. J Clin Invest. 1997; 100:2310–2314. [PubMed: 9410909]

12. Shahani S, Braga-Basaria M, Maggio M, Basaria S. Androgens and erythropoiesis: Past and present. J Endocrinol Invest. 2009; 32:704–716. [PubMed: 19494706]

13. Choi HK, Mount DB, Reginato AM. Pathogenesis of gout. Ann Intern Med. 2005; 143:499–516. [PubMed: 16204163]

14. Bleyer AJ, Trachtman H, Sandhu J, et al. Renal manifestations of a mutation in the uromodulin (Tamm Horsfall protein) gene. Am J Kidney Dis. 2003; 42:1–7.

15. Pentz ES, Moyano MA, Thornhill BA, et al. Ablation of renin-expressing juxtaglomerular cells results in a distinct kidney phenotype. Am J Physiol Regul Integr Comp Physiol. 2004; 286:474–483.
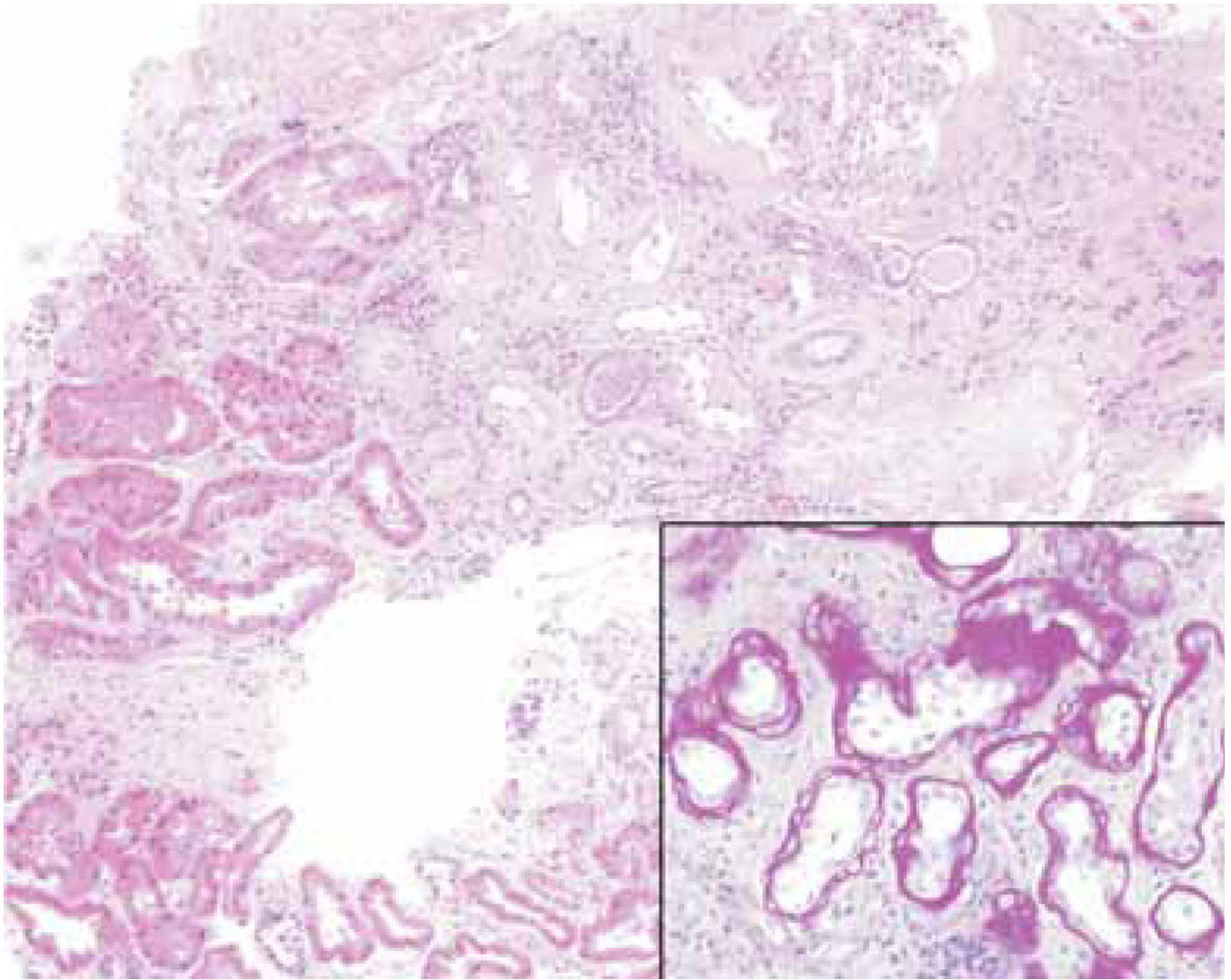
16. Vylet'al P, Kubiova M, Kalbacova M, et al. Alterations of uromodulin biology: A common denominator of the genetically heterogeneous FJHN/MCKD syndrome. Kidney Int. 2006; 70:1155–1169. [PubMed: 16883323]

17. Guidi E, Giglioni A, Cozzi MG, Minetti EE. Which urinary proteins are decreased after angiotensin converting enzyme inhibition? Renal Failure. 1998; 20:243–248. [PubMed: 9574449]

18. Ying WZ, Sanders PW. Dietary salt regulates expression of Tamm-Horsfall glycoprotein in rats. Kidney Int. 1998; 54:1150–1156. [PubMed: 9767530]

Figure 1.
Pedigree and DNA analysis. A: Family pedigree. Black symbols denote affected individuals, open symbols denote unaffected individuals. Analyzed STR (short tandem repeats) markers, corresponding genotypes and reconstructed haplotypes are provided for each individual. B: Chromatograms showing genomic DNA sequence of the *REN* exon 1 in control and a heterozygous transition c.58T > C in patient AIII2.
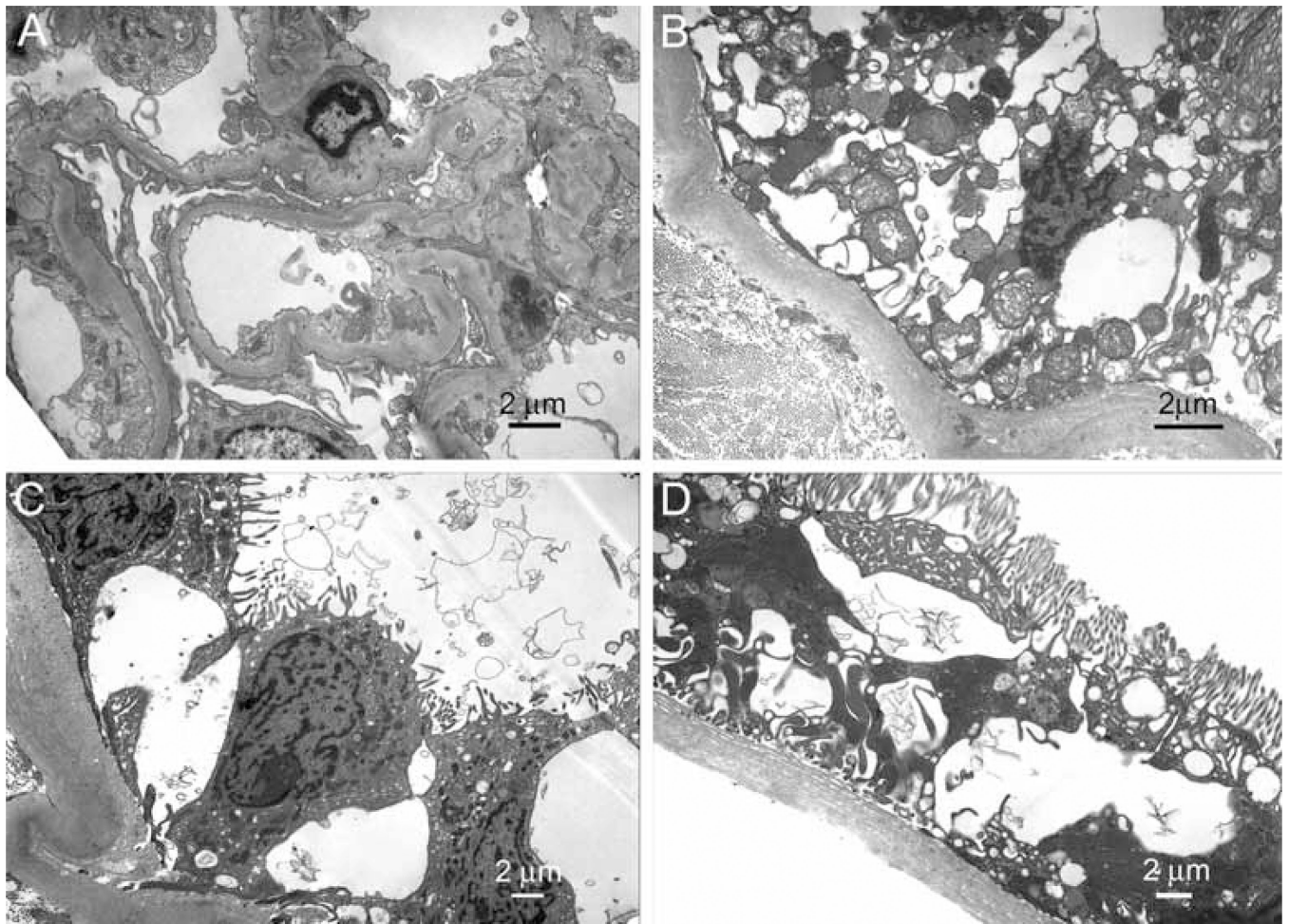
Figure 2.
Estimated glomerular filtration rate vs. age in affected family members.

Figure 3.
Renal biopsy (Hematoxylin and eosin stain). Kidney biopsy of patient AII6 reveals patchy interstitial fibrosis accompanied with focal chronic inflammatory infiltrate, and focal tubular atrophy with markedly thickened and duplicated basement membranes (insert, periodic acid-Schiff). Focal proximal tubules showed hypertrophy. Only one glomerulus was present and showed periglomerular fibrosis but no other alterations by light microscopy.
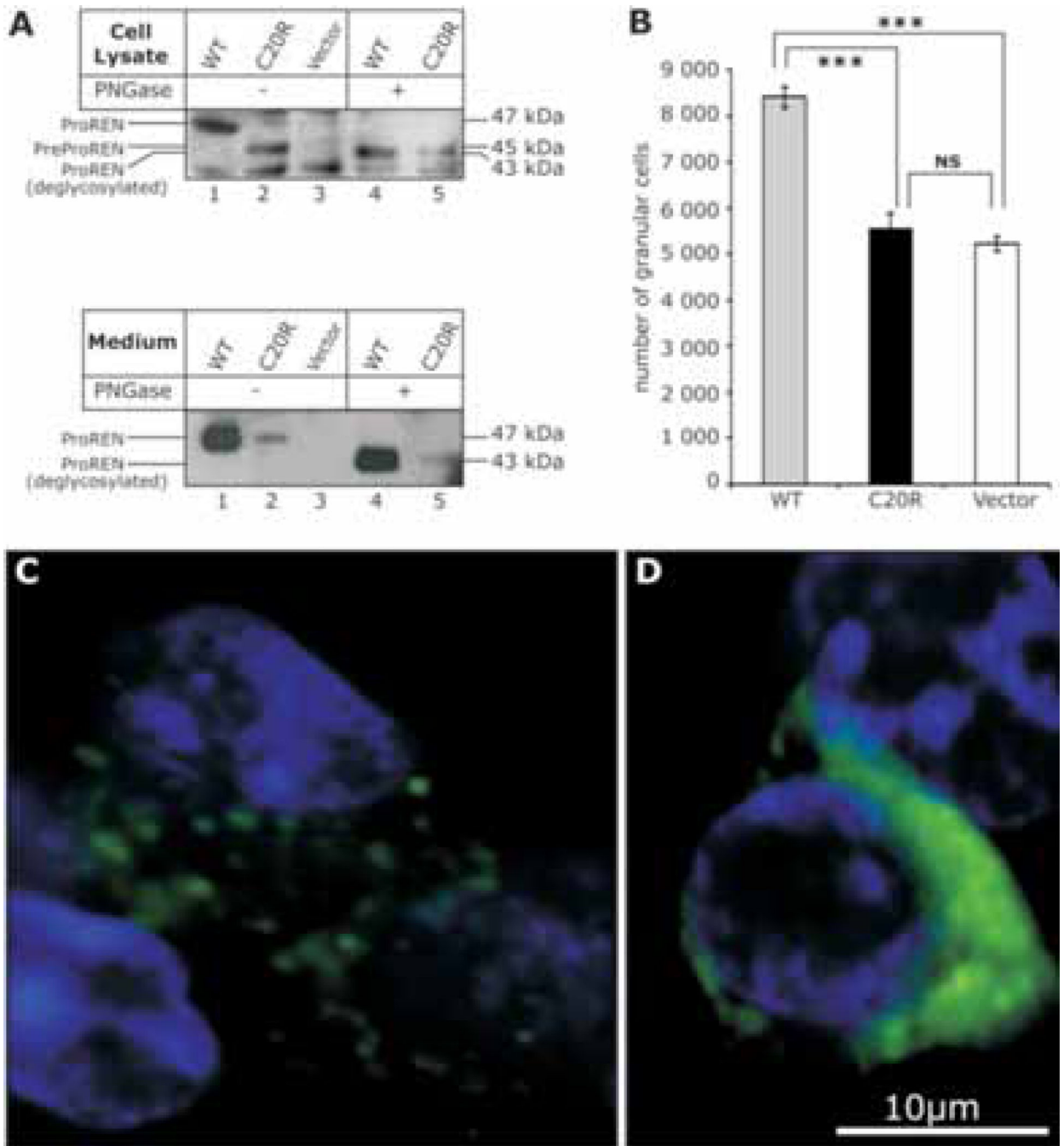
Figure 4.
Ultrastructural examination of kidney biopsy specimen from patient AII6. A: Glomerulus with segmentally thickened and homogenous basement membranes. Segmental podocyte foot process effacement was present. B: Epithelial cells of proximal tubule demonstrating distention of basal membrane invaginations and thickening of tubular basement membrane. C: Distal tubule with marked distention of the intercellular spaces between epithelial cells and thickening of tubular basement membrane. D: Proximal tubule showing epithelial cell atrophy without any significant reduction of the brush border. Thickening of tubular basement membrane and distention of basal membrane invaginations are also present.
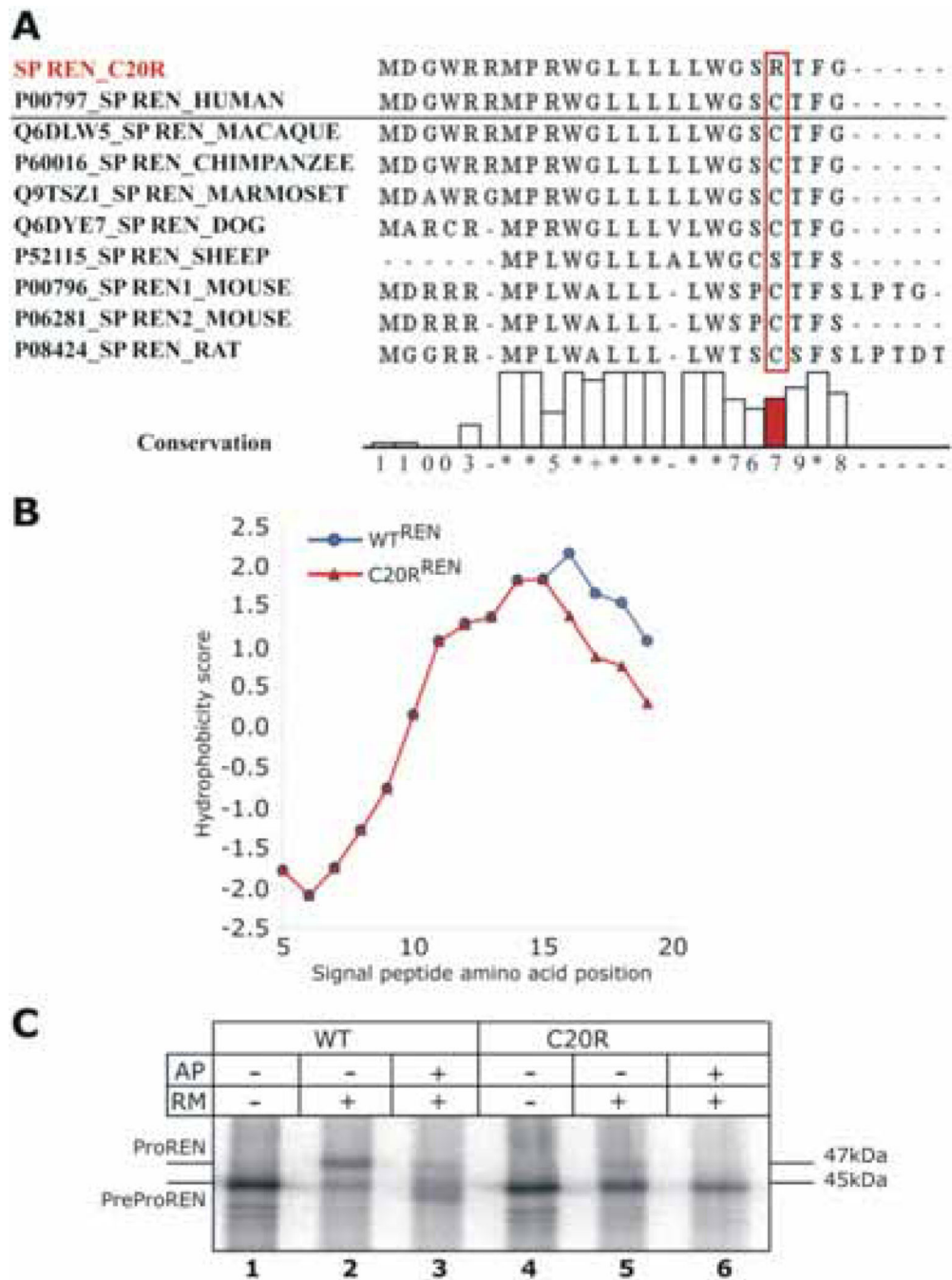
Figure 5.
Bioinformatic and in vitro characterization of mutant renin. A: Amino acid conservation of renin signal sequence across higher mammals. B: Hydrophobicity scores for the wild type and mutated preprorenin signal peptides. C: Nascent WT[REN] and C20R[REN] proteins translated in vitro from corresponding mRNAs in nuclease-treated rabbit reticulocyte lysate in the absence (–) or presence (+) of rough endoplasmic reticulum microsomes (RM) and tripeptide glycosylation acceptor (AP). Without RM and AP only nascent preprorenin (PreProREN) is formed (lanes 1 and 4). With RM and in the absence of AP most of the ER-

translocated WT^{REN} is converted into fully glycosylated prorenin (ProREN); (lane 2) whereas C20R^{REN} produces only minute amounts of ProREN (lane 5). With RM and AP, the glycosylation of the ER-translocated WT^{REN} is inhibited and partially glycosylated intermediates are present (lane 3); C20R^{REN}, which is not ER-translocated, is present as non-glycosylated preprorenin.
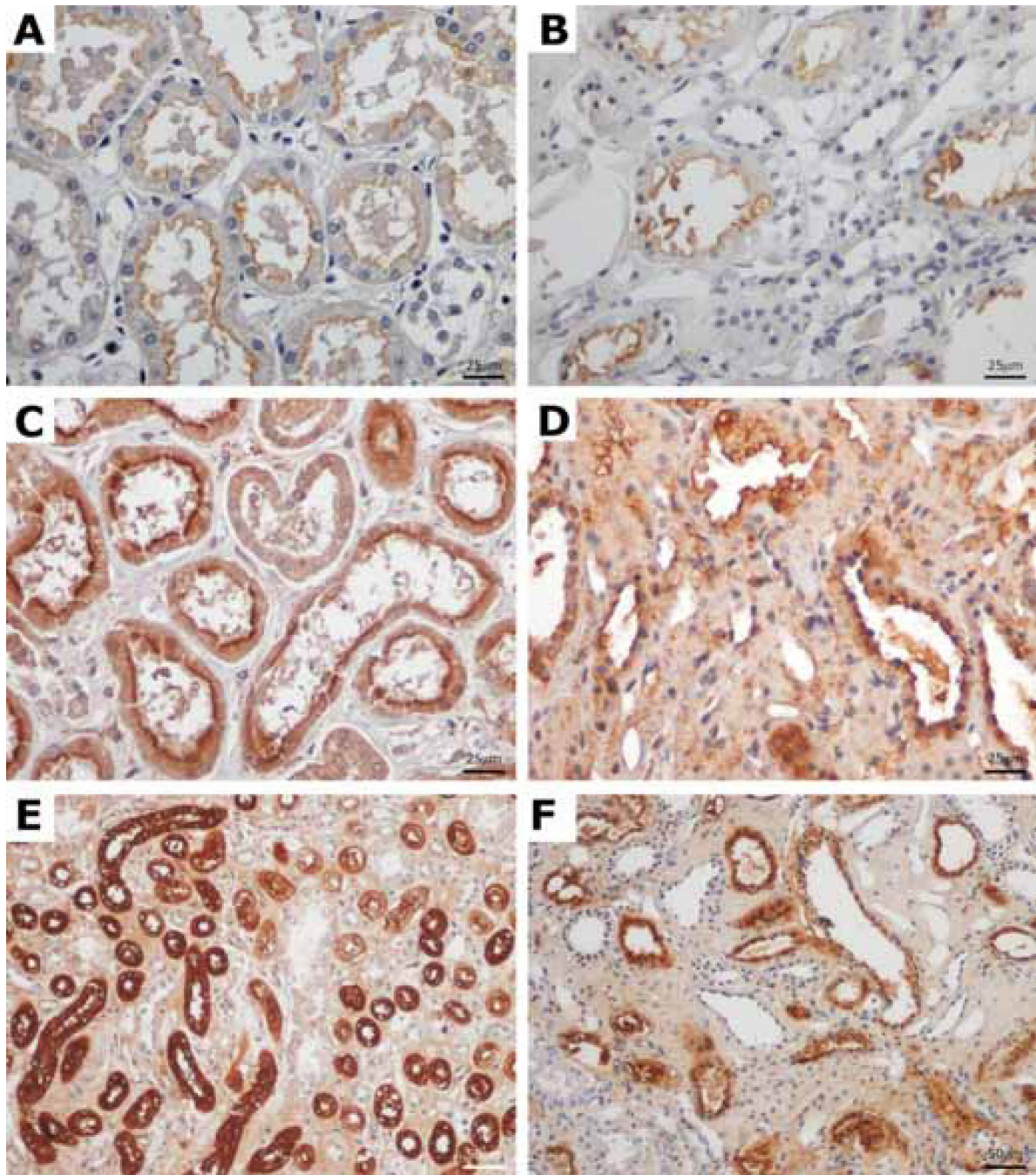
Figure 6.
Transient expression of WT[REN] and C20R[REN] preprorenin in HEK-293 cells. A: Western blot analysis of the protein products in cell lysates and medium showing that C20R[REN] produces only minute amounts of normally glycosylated, proteolytically processed and secretory competent prorenin (ProREN). To distinguish proteolytic processing and glycosylation status, the expressed proteins were analyzed before (–) and after (+) deglycosylation with PNGase. B: Fluorescence-activated cell sorter analysis showing inability of the C20R[REN] to form cytoplasmic granules. The values represent means ± s.d. of

the three transfection experiments carried out in triplicates. The differences between the number of granular cells expressing the WT^{REN} and cells expressing either the C20R^{REN} or empty vector were statistically significant (p < 0,001). C,D: Cellular localization of preprorenin, prorenin and renin in HEK293 cells detected using antibodies recognizing amino acid residues 288 – 317 of the preprorenin (Yanaihara, Shizuoka, Japan). C: WT^{REN} is present in a form of fine cytoplasmic granules. D C20R^{REN} protein is retained intracellularly and shows intense diffuse cytoplasmic staining.

Figure 7.
Immunohistochemical analysis of selected RAS components and UMOD performed in kidney biopsy from Patient AII6. Comparison with age matched control. A: Angiotensin converting enzyme 1 (ACE 1) expression at the apical pole of proximal tubules in a control kidney. B: ACE 1 positivity almost comparable with the control in partly atrophic proximal tubules in patient's kidney. C: Angiotensin II (ANG II) positivity at the apical pole of proximal tubules and in tubular fluid in a control kidney. D: Slightly decreased ANG II staining intensity in patient's kidney revealing also tubular atrophy and interstitial fibrosis.

E: Control kidney characterized by strong uromodulin (UMOD) expression in TALH, with some variability of staining intensity. F: Markedly decreased UMOD positivity in areas of pronounced tubulointerstitial changes in patient's kidney. Maximal UMOD expression was seen at the apical pole of TALH in both, patient and control.

Table 1

Fludrocortisone administration.

Participant	Time	Blood pressure (mm Hg)	Weight (lbs.)	Serum Na (mEq/l)	Serum K (mEq/l)	BUN (mg/dl)	Serum creatinine (mg/dl)	Serum uric acid (mg/dl)	Fractional excretion urate (%)	Urine volume (ml)	Urine Na (mEq/24h)
AIII2	– 11 weeks	87/50		137	5.0	49	1.3	3.2		1,825	69
	– 1 week		87.6	137	5.6	62	1.6	5.2		2,275	
	1 week	106/69	90	142	4.2	26	1.1	6.1	5.1	2,450	72
	6 weeks	112/67		143	4.3	31	1.0	7.0	3.9	2,675	70
	4 months			143	4.5	27	1.1	6.4			
	7 months			142	4.3	28	1.2	6.7			
AII6	0	130/78	201.4	138	4.7	42	1.9	6.1	3.3	3,150	91
	Day 3	118/88	201.6	139	4.3	43	2.0	5.9	4.4	3,450	98
	Day 7	115/81	201.2	140	4.4	42	1.9	6.3	4.2	2,800	81
	Day 8	152/101	203							4,650	
BII4	0	126/84	206	144	5.2	28	1.6	7.5	4.8	1,825	106
	Day 3	117/85	204.9	143	3.9	29	1.8	8.2	4.8	1,750	103
	Day 7	95/70	204.5	144	4.8	30	1.7	9	4.4	1,700	77
	Day 8	122/86	206.4							1,800	

NIH-PA Author Manuscript

NIH-PA Author Manuscript

NIH-PA Author Manuscript

Table 2

Overnight urine osmolality in two families with different renin mutations.

Mutation	Gender	Age (years)	eGFR (ml/min/ 1.73 m^2)	Overnight urine osmolality (mOsm/kg)	Osmolality measurements
C20R^{REN}	Female	10	75	367.7 ± 24.4	3
C20R^{REN}	Male	43	41	426.6 ± 0.7	2
L16^{REN}	Female	9	Not obtained	1,063	1
L16^{REN}	Male	32	58	498 ± 33.2	2